

Electric Polarization of Dilute Polar Solutions: Revised Treatment for Arbitrary Shaped Molecules

Ivan Vlasiouk and Sergei Smirnov*

Department of Chemistry and Biochemistry, New Mexico State University, Las Cruces, New Mexico 88003

Received: January 14, 2003; In Final Form: May 29, 2003

A model for deducing dipole moments of solute molecules from the electric polarization of dilute solutions is revised. The treatment represents a modified Onsager model extended toward arbitrary-shaped molecules. A simplified approach for data evaluation is suggested and compared with the analytical solution for an ellipsoidal cavity and with a numerical solution for two spherical ions.

Introduction

Onsager's semicontinuum model¹ is widely used for treating solvent effects in various situations² ranging from the calculation of reorganization and solvation energies to evaluation of dielectric properties of solutions. In this model, a molecule is represented as a point dipole that is placed in the center of a spherical cavity of radius a (representing the molecule) and surrounded by a dielectric continuum with the dielectric constant of a solvent, ϵ . Solvent polarization by the dipole leads to a reaction field, R

$$R = f\mu = \frac{1}{a^3} \frac{2(\epsilon - 1)}{2\epsilon + 1} \mu \quad (1)$$

that in turn polarizes the molecule. This results in an enhanced molecular dipole moment, μ'

$$\mu' = \frac{\mu_g}{1 - f\alpha} = \frac{\mu_g}{1 - \frac{\alpha}{a^3} \frac{2(\epsilon - 1)}{2\epsilon + 1}} \quad (2)$$

where μ_g is the molecule's gas-phase dipole moment and α is its polarizability. The electric polarization of a solution can be calculated using the orientational distribution functions, $W(\theta)$, for the solute and solvent dipole moments. The functions $W(\theta)$ (for each type of dipoles) are related to a Boltzman distribution of the dipole energy, $U(\theta)$, in the external field

$$W(\theta) = e^{-U(\theta)/kT} \quad (3)$$

where the angle θ is given with respect to the field. In the Onsager model, the dipole energy is equal to the interaction energy of the molecules' point dipole moment with the field inside the cavity, E_c

$$U(\theta) = -(\vec{\mu}' \cdot \vec{E}_c) = -\mu' \cdot E_c \cos \theta \quad (4)$$

For a spherical cavity, E_c is equal to

$$(\vec{E}_c)_{\text{spherical}} = \frac{3\epsilon}{2\epsilon + 1} \vec{E}_0 = \xi_{\text{sph}} \vec{E}_0 \quad (5)$$

In the Onsager model, interaction of the dipole with other surrounding dipoles is neglected apart from the effect of changing the cavity field. The average dipole moment will have a nonzero projection along the external field, which, in the limit of small external fields, can be calculated as a sum of an orientational part

$$\langle \vec{\mu} \rangle = \int \vec{\mu}' e^{-U(\theta)/kBT} d\Omega = \int \vec{\mu}' \left(1 + \frac{(\vec{\mu}' \cdot \vec{E}_c)}{k_B T} \right) d\Omega = \frac{\mu'^2}{3k_B T} \vec{E}_c \quad (6)$$

and a polarizability part, $\alpha' E_c$. The total electric polarization, P , which is a measure of the average dipole moment per unit volume of the solution, is equal to

$$P = (E_c)_o n_o \left(\alpha'_o + \frac{\mu_o'^2}{3k_B T} \right) + (E_c)_s n_s \left(\alpha'_s + \frac{\mu_s'^2}{3k_B T} \right) \quad (7)$$

where n_o and n_s are solvent and solute number densities, respectively. Imposing a constraint that the total volume is a sum of the volumes of the components leads to the derivation⁴⁻⁶ of an expression for the electric polarization of a dilute solution in the external electric field, E_0

$$P = P'_o + \sum \varphi_s n_s \left(\alpha'_s + \frac{\mu_s'^2}{3k_B T} \right) E_0 \quad (8)$$

where P'_o is the polarization of the neat solvent scaled for the change in volume due to the dissolved solutes. The factor φ_s

$$\varphi_s = \left(\frac{3\epsilon}{2\epsilon + 1} \right)^2 \frac{(2\epsilon + n_D^2)^2}{3(2\epsilon^2 + n_D^4)} \quad (9)$$

depends not only on the solvent dielectric constant but also on its refractive index, n_D . The summation in eq 8 is extended over all types of solutes.

Since the reaction field (eq 1) is much stronger than typical external fields, the dipole moment μ' in eq 2 can be interpreted as the dipole moment of the solute in a particular solvent. With such an interpretation, the measurement of the solution's dielectric constant provides a straightforward method for obtaining an 'unambiguous' dipole moment value for the solute. Moreover, when measuring the dipole moment change due to photoexcitation (as is in the photoinduced transient displacement

* To whom correspondence should be addressed. E-mail: snsm@nmsu.edu.

current technique^{4–6}), the change of the electric polarization shows no dependence on the molecular radius, a . This makes the technique attractive for analyses of photoinduced electron-transfer processes as a ‘direct’ method for measuring the dipole moment change.

Following Böttcher,² we previously tried to extend this analysis to a broader class of nonspherical molecules by treating them as ellipsoids and scaling appropriately the local field factor inside a nonspherical cavity.^{4–6} As discussed below, this extension did not take into account the effect of solvent polarization. Here we correct this shortcoming and suggest an approximate method for treating generic molecular shapes.

Theory

Onsager’s model prescribes that the potential energy $U(\theta)$ in eq 3 can be reduced to that of a point dipole interaction with the external field modified by surface charges on the interface between the cavity and the surrounding solvent. The resulting description can be simplified to introducing a new cavity field, E_c , on the solute’s point dipole inside the cavity, with the total energy of that dipole in the external field given by the same eq 4. Kirkwood⁷ pointed out that the assumption of treating the solvent as a continuum in the vicinity of the cavity surface is oversimplifying and could fail when correlations similar to hydrogen bonding exist between molecules. Nevertheless, in many cases, especially when solutes are larger than solvent molecules and no specific interactions are present, this correlation can probably be neglected. One should note that in the case of a spherical cavity, Onsager’s assumption of zero contribution of the solute–solvent interaction to the distribution function in eq 4 is consistent with a zero net polarization induced in the solvent by the solute. Indeed, the integral of the field from a point dipole, E_μ , over the region outside a spherical cavity is exactly zero due to the spherical symmetry

$$\int_{V>V_c} \vec{E}_\mu dV = \oint_{S_c} \varphi_c(r) d\vec{S} = 0 \quad (10)$$

The situation changes when the cavity is nonspherical. First of all, the field inside the cavity is different. For example, in an ellipsoidal cavity with its axis ‘ a ’ oriented parallel to the external field, the field inside equals

$$(\vec{E}_c)_a = \frac{\epsilon}{\epsilon + (1 - \epsilon)A_a} \vec{E}_0 = \xi_a \vec{E}_0 \quad (11)$$

where the ‘depolarization factor’, A_a , is given by the integral^{2–4}

$$A_a = \frac{abc}{2} \int_0^\infty \frac{ds}{(s + a^2)^{3/2}(s + b^2)^{1/2}(s + c^2)^{1/2}} \quad (12)$$

Obviously, eqs 11 and 12 reduce to the spherical case, given by eq 5, when the three semiaxes, a , b , and c , become equal and when $A_a = 1/3$.

Böttcher attempted to extend Onsager’s model to a nonspherical case² via substituting the cavity field in eq 7 by its nonspherical analogue given in eq 11. We followed the same approach in our treatment of the transient displacement current data.^{4–6} There is an intrinsic inconsistency in such an approach. Because of a nonspherical geometry, the integral in eq 10 is no longer zero, i.e. one cannot presume that a dipole moment in an ellipsoidal cavity has zero effect on the orientation of surrounding solvent dipoles.

We will try to resolve this problem by enclosing the solute molecule in a spherical cavity in which the remaining part of

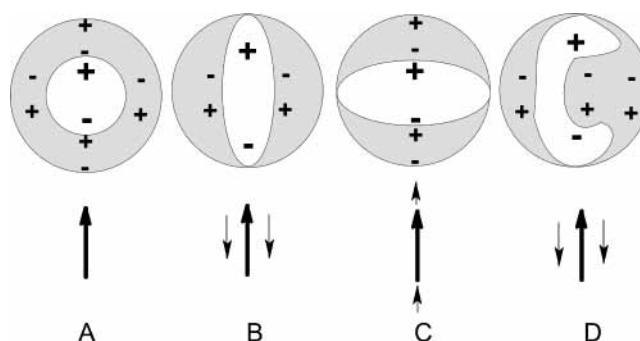


Figure 1. Illustration of solvent-induced dipole moment for different molecular cavity shapes. The molecular cavity is identified by the white region, while the gray area outside it shows solvent enclosed into a larger sized spherical cavity together with the molecule. In the case, A, of a spherical molecular cavity, the solute dipole moment, μ_{cs} , shown by the large plus and minus signs and thick arrow, polarizes solvent in such a way that net dipole moment induced in the solvent, M_s , is zero. Cases B and C represent the prolate and oblate cavity shapes, respectively. Solute dipole of a prolate shape induces dipole moment in the surrounding solvent, M_s (small pluses and minuses and thin arrows), that partially cancels the solute dipole moment, while in the oblate case the solvent induced complements the solute dipole. In a concave molecule (case D) the dipole moment induced in the solvent, M_s , might counteract the solute dipole to an even greater extent than in the prolate case B.

the cavity is filled with a continuum dielectric matching properties of the solvent. This approach is similar to the Kirkwood model⁷ but is much simpler since any short-range-specific interactions in the vicinity of the solute molecule are neglected. This should be an acceptable simplification for large solutes and can be cautiously applied to small molecules as well. We will consider exact solutions to simple molecular cavity shapes and then propose a simplified treatment for arbitrary shaped molecules.

In our model, we describe a total dipole moment from a solute molecule as a superposition of its own dipole moment, μ'_{cs} , and the induced dipole moment in the solvent, M_s

$$M_{cs} = \mu'_{cs} + M_s \quad (13)$$

where μ'_{cs} has the same meaning as in eq 2, i.e., the dipole moment in a particular solution (not the gas-phase value). In this new interpretation, eq 8 for the electric polarization of the solution becomes

$$P = P'_o + \sum \varphi_s n_s \left(\frac{M_{cs}^2}{3k_B T} \right) E_0 \quad (14)$$

where φ_s is given by eq 9 and the polarizability term is omitted. Note that eq 9 was obtained with the assumption that both solute and solvent molecules were spheres. For simplicity, we will continue treating solvent molecules as spheres while nonsphericity of solutes will be incorporated through the solvent contribution to M_{cs} in eq 13.

To calculate the solvent contribution, M_s , the molecule is enclosed in a spherical cavity of a larger size, as in Figure 1. This divides the solvent into two regions: one external to the cavity and one internal to the cavity yet outside the solute cavity (the shaded regions in Figure 1). The radius of the spherical cavity, R , should be large enough that, from the external solvent perspective, the charge distribution is well represented as a point

dipole. In this limit, the integral over the external volume, V_R , equals zero

$$\int_{V > V_R} \vec{E}_\mu dV = \oint_{S_R} \varphi_e(R) d\vec{S} = 0 \quad (15)$$

as it was in eq 10. The solvent contribution, M_s , to the total dipole moment, M_{cs} , can then be calculated through integration of the electric polarization, $\vec{P}(\vec{r})$, outside the molecular cavity

$$\vec{M}_s = \int_{V_R > V_s} \vec{P}(\vec{r}) dV \quad (16)$$

where the integration takes place over the interior solvent region.

The electric polarization can be found by solving Poisson's equation for the electric field

$$\vec{\nabla} \cdot (\epsilon \vec{E}(\vec{r})) = 0 \quad (17)$$

with appropriate boundary conditions for potential at the molecular surface, S_e . These are

$$\left\{ \begin{array}{l} \varphi_i|_{S_e} = \varphi_o|_{S_e} = \epsilon(\vec{n}_{S_e} \cdot \vec{\nabla} \varphi_o)|_{S_e} \\ (\vec{n}_{S_e} \cdot \vec{\nabla} \varphi_i)|_{S_e} \end{array} \right. \quad (18)$$

where φ_i is the electric potential inside the molecular cavity, φ_o is the potential exterior to the molecule, and n_{S_e} is a unit vector normal to the surface. Knowing the electric field distribution, one can calculate the electric polarization via

$$\vec{P}(\vec{r}) = \frac{(\epsilon - 1)\vec{E}(\vec{r})}{4\pi} \quad (19)$$

and use eq 16 to calculate M_s . An effective solute cavity can be constructed by 'rolling' a sphere with hydrogen's van der Waals radius over the molecular surface. The molecule is represented by a superposition of overlapping spheres with appropriate atomic van der Waals radii. This is a standard procedure used in molecular modeling software packages for calculation of such properties as molecular volume; it also eliminates singularities in Poisson's equation.

The procedure described here allows for calculation of the electric polarization, P , of a dilute solution of molecules with known shape and charge distribution. In reality, we usually solve the inverse problem, i.e., extracting information about the charge distribution in a molecule from the measurements of P (or its change as in the dipole technique) in solutions of that molecule. In Onsager's formulation, this inversion is unambiguous because the charge distribution is represented by a point dipole placed in the center of a spherical cavity. When attempting to determine a distribution of charges within a molecule, however, there is inevitably a greater degree of both complexity and ambiguity in the data interpretation process. Indeed, the polarization, P , only contains information about the first moment of the charge distribution. Given this situation, an appropriate goal is to mimic a charge distribution for the solute and then calculate consecutively μ'_{cs} , M_s , and M_{cs} , comparing the last quantity with the experimentally determined value. While the unique solution to this problem is not always possible, it should work well in cases with 100% charge transfer between well recognizable moieties.

In the following, we consider the procedure in detail and evaluate possible approximations. The procedure starts by distributing charges inside a molecular cavity and surrounding that cavity by a continuous dielectric representing the solvent. On the basis of the charge distribution, Poisson's equation can

be solved numerically. This is quite a demanding approach for an arbitrarily-shaped molecule. The first simplification can be achieved by reducing the charge distribution on the molecule to a simpler representation by placing a few point charges at appropriate locations. Calculations show that results of this approximation are sensitive mostly to where the centers of positive and negative charges are placed; the contribution of finer details is insignificant. A second simplification is imposed on how Poisson's equation is solved. It is based on the fact that the electric field from a point charge in a continuum dielectric differs from the field calculated in a vacuum only by a factor of ϵ . The electric field in a vacuum, E_{vac} , from a set of point charges q_i located at the points r_i , is easily calculated without integration

$$\vec{E}_{vac}(\vec{r}) = \sum_i \frac{q_i}{|\vec{r} - \vec{r}_i|^3} (\vec{r} - \vec{r}_i) \quad (20)$$

Approximating the electric field in a dielectric continuum by E_{vac}/ϵ leads to a relatively simple equation for calculating the solvent contribution to the dipole moment, M_s , that can be realized without numerical solution of Poisson's equation

$$\vec{M}_s = \frac{\epsilon - 1}{4\pi} \int_{V > V_s} \vec{E}(\vec{r}) dV \approx \frac{\epsilon - 1}{4\pi\epsilon} \int_{V > V_s} \vec{E}_{vac}(\vec{r}) dV \quad (21)$$

Here $E_{vac}(\vec{r})$ is calculated according to eq 20 and the integration excludes the molecule's cavity volume, V_s . The integration in eq 21 can be limited from above by a spherical cavity of a large enough radius.

In the following part we will compare analytically and numerically solvable cases with this approximation. If both sides of eq 21 are multiplied by $(1 - 1/\epsilon)^{-1}$ the resulting relationship

$$\frac{\epsilon}{\epsilon - 1} \vec{M}_s \approx \frac{1}{4\pi} \int_{V > V_s} \vec{E}_{vac}(\vec{r}) dV \quad (22)$$

not only reflects the accuracy of the described approximation but also provides a simple mechanism for evaluating the applicability of the concept. According to this equation, the exact value of M_s multiplied by $(1 - 1/\epsilon)^{-1}$, should be equal to M_s in a vacuum, independent of ϵ .

Examples. (1) *Ellipsoidal Cavity.* An ellipsoidal cavity represents a first complication beyond the spherical cavity model. This cavity can be characterized by three semi-axes: a , b , and c . Poisson's equation, in this case, can be solved analytically, which is also useful here because it allows for evaluation of the approximations in eq 22. Figure 2 represents plots of equipotential surfaces obtained by numerical solution of Poisson's equation using the FEMLAB program.⁹ The comparison illustrates that the exact solution looks very similar to the 'vacuum solution' of eq 20 normalized by the dielectric constant. Quantitative assessment of the accuracy of our approximations is given in Figure 3, where the exact solution for M_s is shown as a function of the dielectric constant for the ellipsoid of Figure 2. The numerical solutions, given by points, are in essentially exact agreement with the analytical solution

$$M_s = -\frac{(1 - 3A_a)(\epsilon - 1)\mu}{\epsilon + (1 - \epsilon)A_a} \frac{\mu}{3} \quad (23)$$

where the depolarization factor, A_a , is given by eq 12. From the analytic solution in eq 23 it is apparent that the solvent

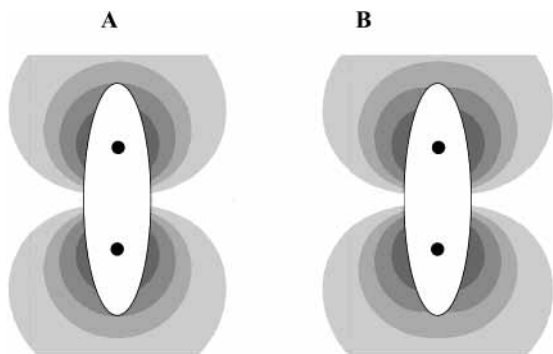


Figure 2. Two-dimensional projection of the 3-D isopotential surfaces normalized by the dielectric constant, ϵ , for two point charges of opposite sign placed at the foci of a spheroid with the aspect ratio $a/b = 3.5$. The dielectric constant outside the ellipse is $\epsilon = 1$ and 10 for cases A and B, respectively, but inside the spheres is unity in both cases. Note that if scaled by ϵ , the two solutions are very similar. Regions with potentials 0.05, 0.1, and 0.15 (in units charge/distance) are shown in three different colors.

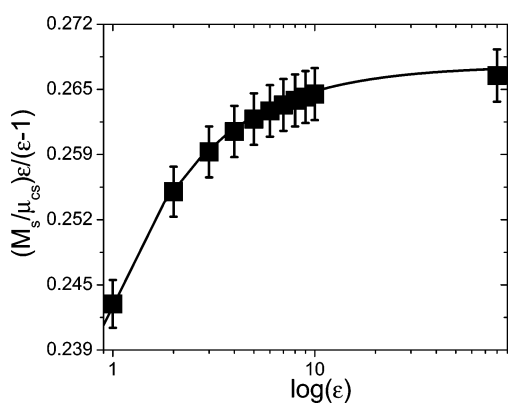


Figure 3. Integrated solvent-induced dipole moment dependence on the dielectric constant ϵ for the case of Figure 2. Points are calculated numerically using Femlab program (see text for details). Solid line represents the analytic solution of eq 23 with $A_a = 0.08965$.

contribution is negative for prolate molecules ($A_a < 1/3$) and becomes positive for oblates ($A_a > 1/3$). As Figure 3 indicates, the E_{vac}/ϵ approximation works well for a prolate ellipsoid. The maximum error can be characterized by the spread between the maximum and minimum values in Figure 3. Taking advantage of the analytic solution, we can evaluate that error as

$$\Delta \left[\frac{\epsilon}{(\epsilon - 1)} M_s \right]_1^\infty = \left(\frac{1}{3} - A_a \right) \mu \left[\frac{A_a}{1 - A_a} \right] \quad (24)$$

which is negative for oblate spheroids (or any ellipsoid with dipole moment oriented along short axis) and can be quite large. For prolate spheroids the error is positive (overestimate in the resulting μ_{cs}) and quite small—the largest error for $A_a < 1/3$ is less than 3.4% and is realized for $A_a = 0.1835$. A negative and plausibly large error for molecules with dipole moment oriented along a short axis, such as oblate spheroids, has to be noted too. However, molecules of this type are rare and using an ellipsoidal approximation for them would be a better choice, as compared with the use of approximation 21.

Combination of eqs 13, 14, and 23 simplifies to a more compact form

$$P = P'_o + \sum \varphi_c n_s \left(\frac{\mu'_{cs}}{3k_B T} \right) E_0 \quad (25)$$

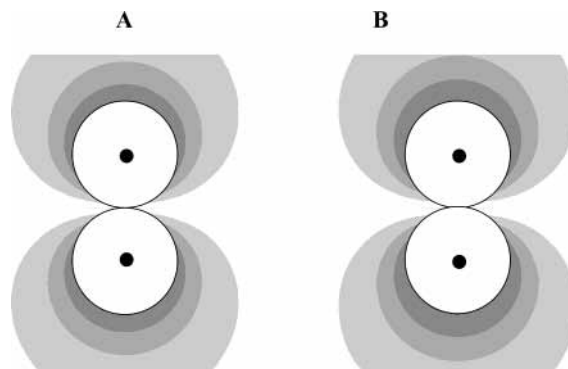


Figure 4. Two-dimensional projection of the 3-D isopotential surfaces normalized by the dielectric constant, ϵ , for two point charges of opposite sign placed inside the two spheres of equal radii that are positioned at close contact. The dielectric constant outside the spheres is $\epsilon = 1$ and 10 for cases A and B, respectively, but inside the spheres is unity in both cases. Note that if scaled by ϵ , the two solutions are very similar. Regions with potentials 0.05, 0.1, and 0.15 (in units charge/distance) are shown in three different colors.

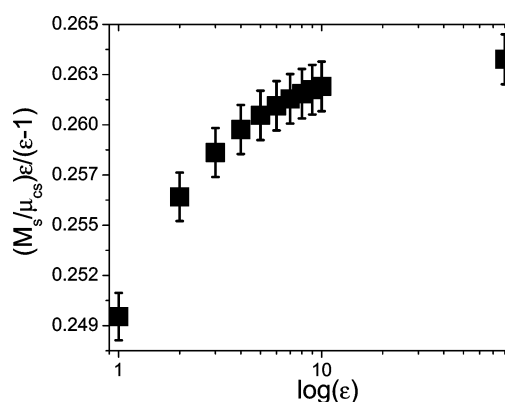


Figure 5. Integrated solvent-induced dipole moment dependence on the dielectric constant ϵ for the case of Figure 4. Points are calculated numerically using Femlab program (see text for details).

with a new factor, φ_c

$$\varphi_c = \left(\frac{\epsilon}{\epsilon + (1 - \epsilon)A_a} \right)^2 \frac{(2\epsilon + n_D^2)^2}{3(2\epsilon^2 + n_D^4)} = \xi_a^2 \frac{(2\epsilon + n_D^2)^2}{3(2\epsilon^2 + n_D^4)} \quad (26)$$

This compact form offers a more straightforward interpretation—the dipole moment $\xi_a \mu'_{cs}$ is the ‘external dipole moment’ introduced by Onsager and now extended for a nonspherical cavity. Alternatively, one may relate the two dipole moments, μ'_{cs} and M_{cs} , as a measure of solute nonsphericity, η_a , given by

$$\eta_a = \frac{\mu'_{cs}}{M_{cs}} = 3 \frac{\epsilon + (1 - \epsilon)A_a}{2\epsilon + 1} = \frac{\xi_{sph}}{\xi_a} \quad (27)$$

(2) *Two Spheres.* This model is a natural approximation for intermolecular charge separation. The two-sphere case is relatively easy to solve numerically using the FEMLAB program.⁹ In Figure 4, isopotential surfaces normalized by the dielectric constant, ϵ , for two point charges of opposite sign placed inside two spheres of equal radii in contact are shown. The dielectric constant outside the spheres is $\epsilon = 1$ and 10 for cases A and B, respectively, but inside the spheres is unity in both cases. Visually it is difficult to recognize a difference between the two graphs. Qualitative comparison is given in Figure 5 for spheres in contact, while Figure 6 illustrates it for two identical spheres separated by one radius. As before

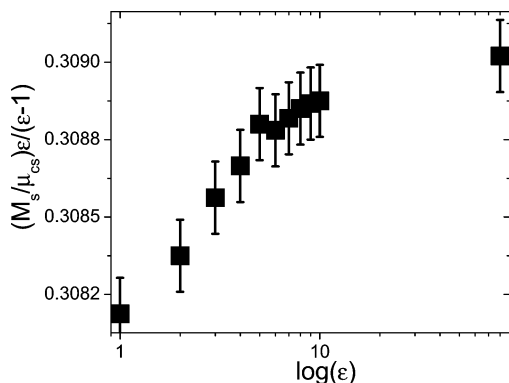


Figure 6. Integrated solvent-induced dipole moment dependence on the dielectric constant ϵ for the case when two point charges of opposite sign are placed inside the two spheres of equal radii that are positioned at a distance three times their radii. Points are calculated numerically using Femlab program (see text for details). Note that the dependence is weaker than that in Figure 5 for charges in close proximity.

for a spheroid, a weak dependence on ϵ in Figures 5 and 6 supports the validity of the estimate in eq 21. The spread of M_s is smaller when the ions are further separated, as expected from the model, but even for close contact the spread is less than 2.6%.

Thus, we see that in cases where analytic and numeric solutions allow comparison of exact values for solvent contribution, M_s , to the dipole moment with that approximated using eq 21, the agreement is acceptable given the enormous simplification of numeric solution. Prolate molecules are treated exceptionally well in this model, while oblate molecules and molecules where dipole moments oriented along short axes have to be approached more cautiously. It helps to realize that the latter cases are very rare or typically of low interest. It is also worth noting that extremely prolate molecules ($A_a \sim 0$) or any other case where the distance between separated charges defines a sphere with the volume much larger than molecule's volume, eqs 25 and 26 reduce to a much simpler form for the coefficient φ_c

$$\varphi_c = \frac{(2\epsilon + n_D^2)^2}{3(2\epsilon^2 + n_D^4)} \quad (28)$$

This simplification might be very useful for large molecules where ellipsoidal approximation is difficult to apply.

Experimental Examples

This paper is dedicated primarily to establishing an improved theoretical treatment for analysis of dielectric polarization data and the transient displacement current data in particular. Below we give a few examples as a demonstration of consequence for the revised treatment. The measurements were performed using our standard setup for the transient displacement current measurement, the details of which can be found elsewhere.⁶

Almost Spherical Molecules. Bianthryl is an interesting symmetric molecule, which gains a dipole moment upon photoexcitation by 'breaking' its ground-state D_{2d} symmetry. Nevertheless, the excited-state D_2 distortion is not very dramatic. The excited state of this molecule possesses a dipole moment even in nonpolar solvents such as toluene. Even though the spherical model was used to evaluate its dipole moment,¹² neither a spherical nor an ellipsoidal approximation describes well the molecule's shape. As a result, the approximate method of eqs 20 and 21 is appropriate. For this purpose, a program

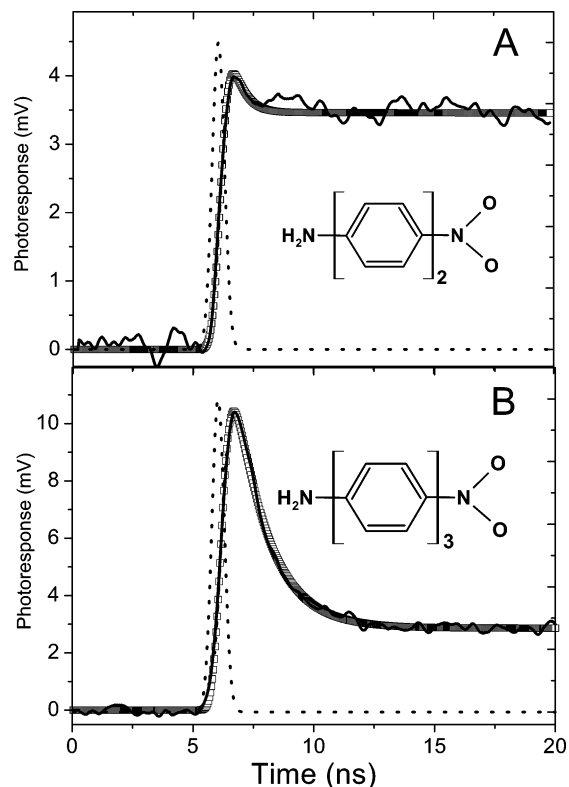


Figure 7. Transient displacement current signals for two molecules in toluene solution observed after absorbing $38 \mu\text{J}$ at 396 nm in a cell with a 0.56 mm gap and using a $1 \text{ M}\Omega$ load resistor. The experimental traces are shown by solid lines and the fitting curves by points; dashed lines depict laser pulse. (A) PANB. Simulation was done with the following parameters: $M_{cs} = 18.5 \text{ D}$, the lifetime of a singlet charge-transfer excited state $\tau_{CRS} = 0.7 \text{ ns}$, and the intersystem crossing to a long-lived triplet charge transfer state $\tau_{isc} = 0.6 \text{ ns}$. (B) PANT. Simulation parameters: $M_{cs} = 29.3 \text{ D}$, $\tau_{CRS} = 1.7 \text{ ns}$, $\tau_{isc} = 8.3 \text{ ns}$.

was written in FORTRAN 90 which calculates the solvent contribution to the dipole moment, M_s , from eq 21. Charges in the dipolar state of bianthryl were distributed according to charge densities in the cation and anion radicals of the two anthracene moieties, respectively. This distribution corresponds to the dipole moment $\mu'_{cs} = 20.6 \text{ D}$. Using van der Waals radii from Bondi⁸ we calculated $M_s = -3.86(1-1/\epsilon) \text{ D}$. This leads to a 10–20% reduction of the dipole moment, depending on the solvent polarity.

Almost Ellipsoidal Molecules. DMANS, 4-dimethylamino-4'-nitrostilbene, is a molecule that has been frequently used for calibration and comparison using different methods.^{4,6,11} Previously we reported that in the spherical approximation, DMANS' dipole moment in toluene equals $M_{cs} = 31.0 \pm 1.5 \text{ D}$.⁶ Due to the elongated and rigid shape of this molecule, the ellipsoidal approximation seems appropriate for DMANS. Using the ground-state geometry obtained by semiempirical AM1 optimization, the following semiaxes were calculated:¹⁰ $a = 11.8 \text{ \AA}$, $b = 4.1 \text{ \AA}$, $c = 4.1 \text{ \AA}$ with the dipole moment oriented along the a axis. The depolarization factor along this axis equals $A_a = 0.092$, and the dipole calculated from eq 27 is $\mu'_{cs} = 36.4 \pm 1.7 \text{ D}$.

Two 'new' molecules, PANT (*p*-amino-nitroterphenyl) and PANB (*p*-amino-nitrobiphenyl) sketched in Figure 7 along with their dipole signals, also have elongated and rigid shapes, justifying the use of the ellipsoidal approximation for them. The dipole signals shown were measured in the displacement charge mode and have a fast and a slow component: the former being

TABLE 1: Parameters for Scaling Using Ellipsoidal Approximation and the Dipole Moments

molecule	ellipsoidal parameters ¹⁰	M_{cs} , D	A_a^a	η_a^b	$\mu_{cs} = \eta_a M_{cs}$, D
DMANS	$a = 8.8 \text{ \AA}$, $b = 3.4 \text{ \AA}$, $c = 2.0 \text{ \AA}$	31.0	0.092	1.174	36.4
PANB	$a = 6.9 \text{ \AA}$, $b = 3.4 \text{ \AA}$, $c = 2.0 \text{ \AA}$	17.8	0.124	1.151	20.5
PANT	$a = 9.1 \text{ \AA}$, $b = 3.4 \text{ \AA}$, $c = 2.0 \text{ \AA}$	29.3	0.088	1.176	34.5

^a Values are calculated for toluene solvent, $\epsilon = 2.38$. ^b From eq 27.

from the short-lived singlet charge-transfer state and the latter from the triplet charge-transfer state populated via intersystem crossing from the singlet state. Dipole moments and the rates of recombination and intersystem crossing were obtained from independently measured fluorescence lifetimes of the singlet states and by presuming that the dipole moments are the same for the singlet and triplet states. The scaling factors for the dipole moments were calculated from eq 27 treating molecules as ellipsoids with semiaxes given in Table 1.

Very Large Molecules. Two triad molecules for which we have measured dipole moments in their photoexcited states can be described as very large molecules. They are methoxyaniline–aminonaphthalimide–dimethylphenyl–naphthalenediimide–octyl (MA-ANI-NI),⁵ synthesized by the M. Wasielewski group, now at Northwestern University, and carotene–porphyrin–fullerene triad,^{13,14} synthesized at Arizona State University. The former was reported⁵ to have 16.3 Å charge separation if the spherical approximation was used. Reevaluation of its dipole moment can be done by using the ellipsoidal approximation¹⁰ since the molecule is fairly straight and rigid. Using values of $V = 679 \text{ \AA}^3$ and $2a = 32.1 \text{ \AA}$, we find $b = 3.2 \text{ \AA}$ and $A_a = 0.068$. This results in a value of $\mu'_{cs} = 93 \pm 7 \text{ D}$ or 19.4 Å of charge separation, which is in remarkable agreement with the expected charge-separation distance based on the center to center distances for the donor (MA) and acceptor (NI) moieties. Another triad, from ASU, has the largest dipole moment ever experimentally measured.¹⁴ The distance between the centers of the donor and acceptor (carotenoid and fullerene), based on molecular modeling, is 34 Å, which corresponds to a dipole moment of 163 D. This would be in poor agreement with the experimental value in the spherical approximation $M_{cs} = 110 \pm 5 \text{ D}$. The ellipsoidal model is inappropriate in this case due to a bow-like contour of the molecule, but because of its extended shape, the reduced form for the scaling factor given in eq 28 can be applied. The resulting value of the dipole moment $\mu'_{cs} = 154 \pm 6 \text{ D}$ is in good agreement with the value obtained by direct numerical approximation for solvent contribution using eqs 20 and 21, $\mu'_{cs} = 156 \pm 6 \text{ D}$. The latter was calculated using van der Waals radii from ref 8, yielding $M_s = -46 \pm 1 \text{ D}$, and the total dipole moment of the charge transfer state: $\mu'_{cs} = M_{cs} - M_s = 110 + 46 = 156 \pm 6 \text{ D}$. In either approach, the dipole moment demonstrates a remarkable agreement with the value estimated from the expected positions of charges in the charge transfer state of this triad.

Conclusions

The problem of dielectric polarization for dilute polar solutions was revisited, and a new treatment based on calculating the solvent contribution to the total dipole moment for solute molecules has been suggested. An analytic solution for ellipsoidal molecular cavities and a simplified approximation for arbitrary-shaped molecules, based on mimicking the electric field as a solution in a vacuum normalized by the dielectric constant (eq 20), have been derived and analyzed. Experimental examples with photoinduced electron transfer show remarkable agreement between the measured dipole moments and those expected from the distance between donor/acceptor moieties.

Acknowledgment. This work was in part supported by grants from the National Institutes of Health (S06 GM 08136-26) and Research Corporation (RI0398). The authors are thankful to Dr. D. Gust for bringing our attention to the problem and providing the triad molecule and its optimized structure, Dr. P. Piotrowiak for providing PANT and PANB molecules; Dr. C. Braun, Dr. I. Sevostianov, Dr. H. Wang, Dr. D. Smith, Dr. M. Newton, and Dr. D. Matyushov for helpful discussions. The authors are also grateful to COMSOL Inc. for providing a trial version of their Femlab software.

References and Notes

- (1) Onsager, L. *J. Am. Chem. Soc.* **1936**, *58*, 1486.
- (2) Böttcher, C. J. F. *Theory of Electric Polarization*; Elsevier: Amsterdam, London, New York, 1973.
- (3) Liptay W. Dipole Moments and Polarizabilities of Molecules in Excited Electronic States. In *Excited States*; Lim, E. C., Ed; Academic Press: New York, 1974; Vol. I, p 129.
- (4) Smirnov, S. N.; Braun, C. L. *J. Phys. Chem.* **1994**, *98*, 1953–1961.
- (5) Smirnov, S. N.; Braun, C. L.; Greenfield, S. R.; Svec, W. A.; Wasielewski, M. R. *J. Phys. Chem.* **1996**, *100*, 12329–12336.
- (6) Smirnov, S. N.; Braun, C. L. *Rev. Sci. Instrum.* **1998**, *69*, 2875–2887.
- (7) Kirkwood, J. J. *Chem. Phys.* **1939**, *7*, 911.
- (8) Bondi, A. J. *Phys. Chem.* **1964**, *68*, 441.
- (9) FEMLAB is a commercial MATLAB-based electromagnetic modeling tool, which employs the finite element method to solve partial differential equations. The linear stationary 3D electrostatics module was used for solving Laplace equation. Meshing was performed using the default settings for “finer” mesh option. To avoid singularities, point sources were introduced to the system via internal FEMLAB function – V_test.
- (10) The longitudinal axis $2a$ is usually easier to identify as the molecule’s length, *i.e.*, the distance between the remote atoms plus their van der Waals radii. The equatorial axis, $2b$, can then be calculated from the van der Waals molecular volume, $V = 4\pi ab^2/3$, the value for which is usually available from molecular modeling software packages, such as HyperChem, Spartan, or Gaussian. Alternatively, for planar conjugated molecules, the shortest semiaxis can be taken $c = 2.0 \text{ \AA}$ and the b value calculated, based on a and c , from the volume: $V = 4\pi abc/3$.
- (11) Smirnov, S. N.; Braun, C. L. *Chem. Phys. Lett.* **1994**, *217*, 167–172.
- (12) Smirnov, S. N.; Braun, C. L.; Ankner-Mylon, S. E.; Grzeskowiak, K. N.; Greenfield, S. R.; Wasielewski, M. R. *Mol. Cryst. Liq. Cryst.* **1996**, *283*, 243–248.
- (13) Kuciauskas, D.; Liddell, P. A.; Lin, S.; Stone, S.; Moore, A. L.; Moore, T. A.; Gust, D. *J. Phys. Chem. B* **2000**, *104*, 4307–4321.
- (14) Smirnov, S. N.; Liddell, P. A.; Vlassioug, I. N.; Teslja, A.; Kuciauskas, D.; Braun, C. L.; Moore, A. L.; Moore, T. A.; Gust, D. *J. Phys. Chem.* **2003**, 7567.